Progress In Electromagnetics Research C, Vol. 121, 127–144, 2022

A Mathematical Approach to the Effect of Mobile Position on Human Head against RF Radiation

Pudipeddi Sai Spandana* **and Pappu V. Y. Jayasree**

Abstract—The proposed work focuses on the mathematical interpretation of Electromagnetic Shielding Effectiveness (ESE) of age-dependent human Head Models (HMs) of seven tissues (Skin, Fat, Bone, Dura, Cerebrospinal fluid (CSF), Gray matter, and White Matter) with the impact of the mobile phone holding position on the RF radiation absorption by the human head. The ESE is first simulated and estimated using the Transmission Line Method approach: a. for only layered human Head Models (HMs) in the absence of mobile position with variation in Oblique Angle of Incidence (OAI) in Transverse Electric Polarization (TEP) and Transverse Magnetic Polarization (TMP), b. in the presence of mobile phone position and Polarization. c. by incorporating the Transparent Conductive Metal Mesh Polyethylene terephthalate (PET) film (Copper grid PET Film) as a shielding material in the presence and absence of Polarization and mobile phone holding positions. The Copper grid PET Film is composed of optical PET film laminated with Copper (Cu) and Nickel (Ni) Transparent Conductive Mesh Coatings (TCMCs) to form a transparent laminated mesh. The radiation absorption characteristic, Specific Absorption Rate (SAR), is evaluated numerically at four Sub-6 GHz frequencies from the obtained ESE data to draw collation at the least SAR absorbed by the age-dependent HMs, considering the water contents of tissues. Out of adult and child HMs, the child HM absorbed the higher RF SAR. However, with the transparent PET/Cu/Ni Laminated Mesh (LM), at 5.47 GHz, the SAR by the brain's white matter in child HM is highest in TEP with no shield considered is 10 W/kg. With transparent LM, the SAR obtained is 2.8e-12 W/kg in TEP in no mobile phone tilt condition at 89° OAI. With the user mobile tilt at 15° and 30°, the SAR absorbed by the brain WM is 2.62e-12 W/kg and 2.1e-12 W/kg, respectively at 89°. Hence, the SAR absorption is the least in any direction (azimuth or elevation) when the mobile phone is tilted to 30° in TE Polarization using the transparent PET/Cu/Ni laminated mesh. Therefore, the usage of transparent PET/Cu/Ni laminated mesh in TE Polarization saw the least SAR absorbed, whether the mobile phone is tilted either towards or away from the head when the mobile phone is moved to 15° or 30° tilted position.

1. INTRODUCTION

The demand for transmission of higher data rates is delving more into the implementation of new communication technologies with each passing day. The Fifth Generation (5G) wireless communication systems link the existing networks with innumerable wireless devices. Due to their shorter propagation range, the mm wavebands are absorbed by tissue water contents in living beings. This shortcoming can be controlled by increasing the cell density, and thereby the power density [1]. Bioelectromagnetics, or the interaction of Electromagnetic Fields (EMFs) with human tissues, is a growing concern with the rise of frequency bands despite the standards set by EMF regulating authorities. The Specific Absorption Rate (SAR) for determining the emitted EMF from the wireless communication devices, especially

Received 16 May 2022, Accepted 1 July 2022, Scheduled 12 July 2022

* Corresponding author: Pudipeddi Sai Spandana (psspandana26@gmail.com).

The authors are with the Department of Electrical, Electronics and Communication Engineering, GITAM School of Technology, GITAM Deemed to be University, Visakhapatnam, India.

mobile smartphones, will no more be a metric for frequencies greater than 6 GHz. The International Commission on Non-Ionizing Radiation Protection (ICNIRP) has revised its guidelines to propose that the frequencies above 6 GHz are delegated to use the absorbed tissue power density as the metric of RF exposure determination. The 5G frequency bands are currently Sub-1 GHz (Low-band), Sub-6 GHz (Mid-band), and Above 6 GHz (mm-Wave bands).

The amount of Radio Frequency (RF) distribution absorbed by the human head depends on the tissue characteristics such as size, geometry, frequency, water content, and Polarization of incident EMF. Evaluating SAR also involves several parameters such as distance between the mobile phone and the head, positions of head and mobile phone, and Polarization. The limited literature on the SAR effect with the angle of incidence of EM wave and mobile position inclusion is available. Under the Sub-6 GHz SAR reduction, the authors in [2] have constructed a multi-layered metamaterial for the reduction of EMF in mobile devices. With the help of Computer Simulation Technology (CST) Microwave Studio, at some frequencies below 6 GHz, the SAR reduction properties are estimated. At 5.872 GHz, the lowest reported SAR was higher than 50%. The authors have investigated the effect of human age (5 to 70 years) on RF exposure at 26 GHz and 60 GHz to analyze the age-dependent power absorption, and tissue heating [3]. The skin thickness and electromagnetic properties are considered to see the age-dependent tissue heating at the mm-Wave band. The authors have investigated from the results that blood ow in tissues and permittivity are the reasons for showing deviation in power density, SAR, and near-surface heating of tissues. The changes in human body temperature are considered for SAR analysis in tissues. The Finite-Difference Time-Domain (FDTD) method and bio-heat equation are used to calculate the effects. Polarization is taken into account while investigating the SAR [4]. The authors in [5] have studied the overexposure of mobile radiation to temperature rise and SAR in 3D HMs of adult and 7-year-old children. The HM was considered to have skin, fat, and bone tissues. Voice calling, texting, and video calling are the three usages studied focusing on EM absorption characteristics. Radiation absorbed was more in voice calling pattern. The different holding positions of mobile phones (cheek and tilt) were studied [6] to analyze the RF EM radiation effects. The SAR absorbed by the head was more in the cheek position than the tilted positions of 15 and 30°. FDTD method and CST simulations were used for SAR computation. All the literature mentioned has studied the amount of SAR absorption and its distribution using software simulations and the effects of many factors on the SAR. However, not all the authors have mathematically analyzed a proper shielding technique to reduce the SAR in human HMs to prevent the RF over-exposure from mobiles, considering tissue water content parameters.

The novelty of the proposed work is to mathematically investigate the effect of mobile position in elevation and azimuth direction along with the oblique angle of incidence of RF EM wave on a seven-layered human head model (adult/child) with the Transmission Line Method at Sub-6 GHz mobile frequencies. The analysis is performed by realizing the Electromagnetic Shielding Effectiveness (ESE) of the human head in the absence and presence of a transparent Laminated Mesh (LM) composed of PET film as shield and transparent conductive mesh coatings (Cu and Ni) in both the Transverse Electric and Transverse Magnetic Polarization (TEP and TMP) mechanisms without and with different mobile phone positions. The SAR absorbed by the White Matter (WM) is assessed finally to reduce the SAR from the mathematical analysis of ESE. Comparisons are drawn for the age-dependent head models with Oblique Angle of Incidence alone and Oblique Angle of Incidence with mobile phone holding positions. The proposed work does not focus on the internal structure of the mobile phone or its antenna design.

2. HEAD SIZE, HEAD MODELS WITH POLARIZATION, AND MATERIALS

2.1. Head Size in Adult and Child, Planar Seven-Layered Head Model with Polarization Consideration, and Head Tissue Thickness

The general dimensions of the head are considered with a variation in height and diameter of the head in an adult and a child as in Table 1 [7, 8].

A planar head model (HM) consisting of seven layers is considered for the mathematical analysis of plane wave ESE, with tissues: Skin, Fat, Bone, Dura, Cerebrospinal fluid (CSF), Gray Matter, and White Matter (WM) [9] because, at the contact point of mobile handset and the ear, the circular arc of the head appears in the form of a straight line. The two infinite media are the air and WM out of all

Table 1. Head height and diameter in head models of adult and child.

Head Model (HM)	Height (cm)	Diameter (cm)
Adult	25	16.01
Child	23.5	14.06

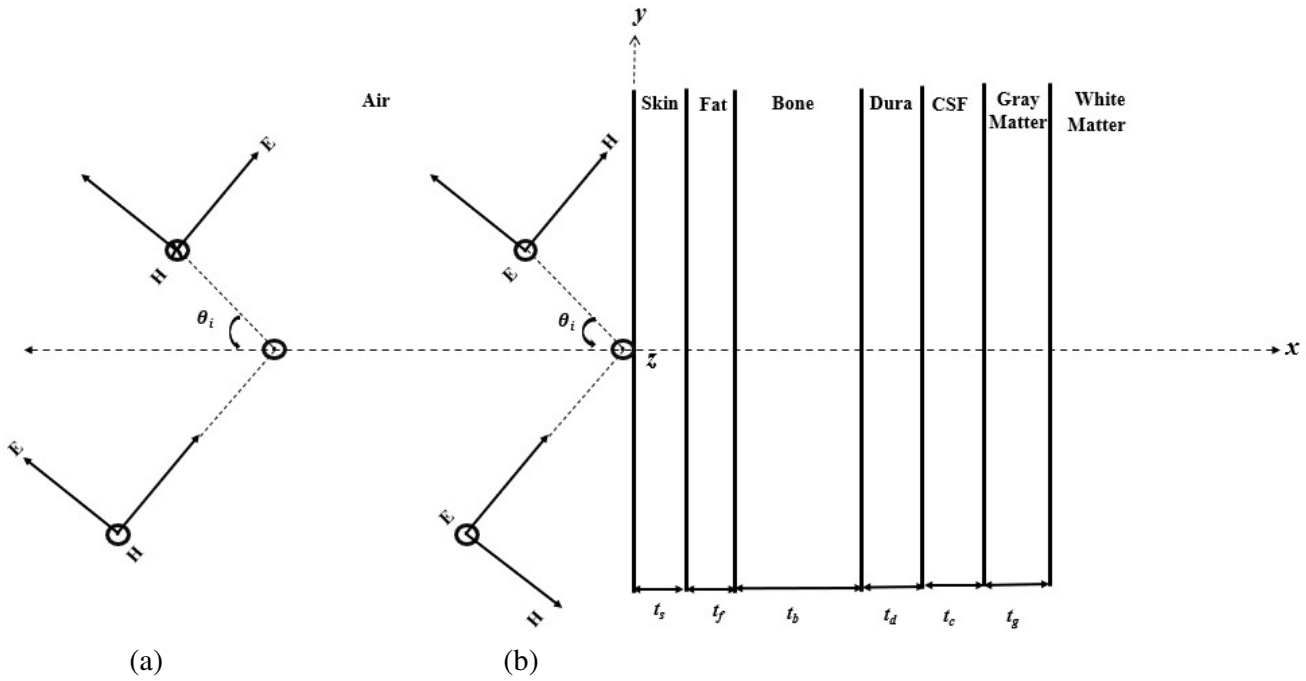

Figure 1. (a) Parallel (TM) Polarization. (b) Perpendicular (TE) Polarization of EM wave incident on air to skin surface of head in a planar seven-layered model of adult/child.

layers. Two Polarization mechanisms are also considered due to the Oblique Angle of Incidence (OAI) of the radiated Electromagnetic (EM) wave on head tissues. Every head tissue has different medium properties such as relative permittivity and conductivity that are variable with the frequency of the incoming EM wave. Let μ_i, ε_i, and σ_i represent the permeability, permittivity, and conductivity of each layered medium. xy axis is the plane of the head with the planar seven layers of the adult/child's head as shown in Fig. 1. $E_x = E_y = 0$ are electric field components of TE wave and $H_x = H_y = 0$ are magnetic components of TM wave. θ_i is the OAI of the ith layer that can range from 0° (worst case or normal incidence) to 90°. The diagram depicts the parallel and perpendicular Polarization of the EM wave with θ_i incident on-air medium. The thickness of each tissue layer starting from Skin, Fat, Bone, Dura, CSF, and Gray matter is indicated in the Table 2 as t_s, t_f, t_b, t_d, t_c, and t_g, respectively.

2.2. Dielectric Properties of Head Tissues

The dielectric properties of the head tissues depend directly on the frequency of the incident wave, tissue size, and, most importantly, water contents in the tissues. The tissue-dependent components are tracked down to compute the complex relative permittivity ($\dot{\varepsilon}_r$) in both the head models. $\dot{\varepsilon}_{rA}$ is the complex relative permittivity of each biological head tissue in an adult, which in turn is dependent on the reference hydration rate (α_C) in the child and the adult (α_A) head tissues. Total Body Water (TBW) is the only age-dependent factor, which is different for adult and child bodies. The TBW is directly and inversely related to hydration rate and tissue mass density. ε_{rw} is relative permittivity of

Table 2. Tissue thickness in a human head model of seven layers [7–9].

Head Model	Tissues	Thickness (mm)
Adult	Skin	1
	Fat	0.5
	Bone	7
	Dura	1.5
	CSF	2
	Gray Matter	3.7
	White Matter	55
Child	Skin	1
	Fat	0.5
	Bone	6.5
	Dura	0.5
	CSF	1.5
	Gray Matter	3.6
	White Matter	56.7

water at 37° which is 74.3 [10]. ε_{rA} is the relative permittivity of adult tissues according to the wave's frequency. τ_A and τ_C are relaxation time constants indicating the manifestation of the Polarization mechanism that characterizes various relaxation regions of the dielectric spectrum in adult and child head tissues, respectively. The relaxation time constants are computed using every tissue's conductivity and relative permittivity at the fixed-mobile frequency from [11]. The water-dependent conductivity of tissues (σ_A and σ_C) are obtained from (3) and (4) in terms of relative permittivity of free space and complex relative permittivity in adult and child head tissues obtained from (1) and (2), respectively.

$$\dot{\varepsilon}_{rA} = \varepsilon_{rw}^{\frac{\alpha_C-\alpha_A}{1-\alpha_A}} \varepsilon_{rA}^{\frac{1-\alpha_C}{1-\alpha_A}} \left(1 - \frac{j}{\omega\tau_A}\right) \tag{1}$$

$$\dot{\varepsilon}_{rC} = \varepsilon_{rw}^{\frac{\alpha_C-\alpha_A}{1-\alpha_A}} \varepsilon_{rC}^{\frac{1-\alpha_C}{1-\alpha_A}} \tag{2}$$

$$\sigma_A = \frac{\varepsilon_0 \dot{\varepsilon}_{rA}}{\tau_A} \tag{3}$$

$$\sigma_C = \frac{\varepsilon_0 \dot{\varepsilon}_{rC}}{\tau_C} \tag{4}$$

2.3. Planar Seven-Layered Head Model after Placement of Transparent Laminated Mesh with Polarization Consideration

The PET film and the Transparent Conductive Mesh Coatings (TCMC), as represented in Fig. 2 are embedded on top of the mobile handset. The transparent conductive Cu and Ni coating form a square mesh structure as in Fig. 3. The shield, along with the transparent conductive coatings as in Fig. 2 constitutes Polyethylene terephthalate (PET) film, laminated with copper and nickel metal mesh. The air gap between the mobile handset and the adult/child head is assumed to be 1 mm. The thickness of PET film and the two TCMCs are represented with t_{sh}, t_{co1}, and t_{co2}, respectively. The same Polarization phenomenon is depicted in Fig. 2 as in Fig. 1, with only difference being the laminated mesh arrangement. The mesh period (g) of the TCMC is 300 µm, and the mesh line width ($2a$) is 7.5 µm [12]. The material forms an Electromagnetic Interference (EMI) shielding layer, protective film,

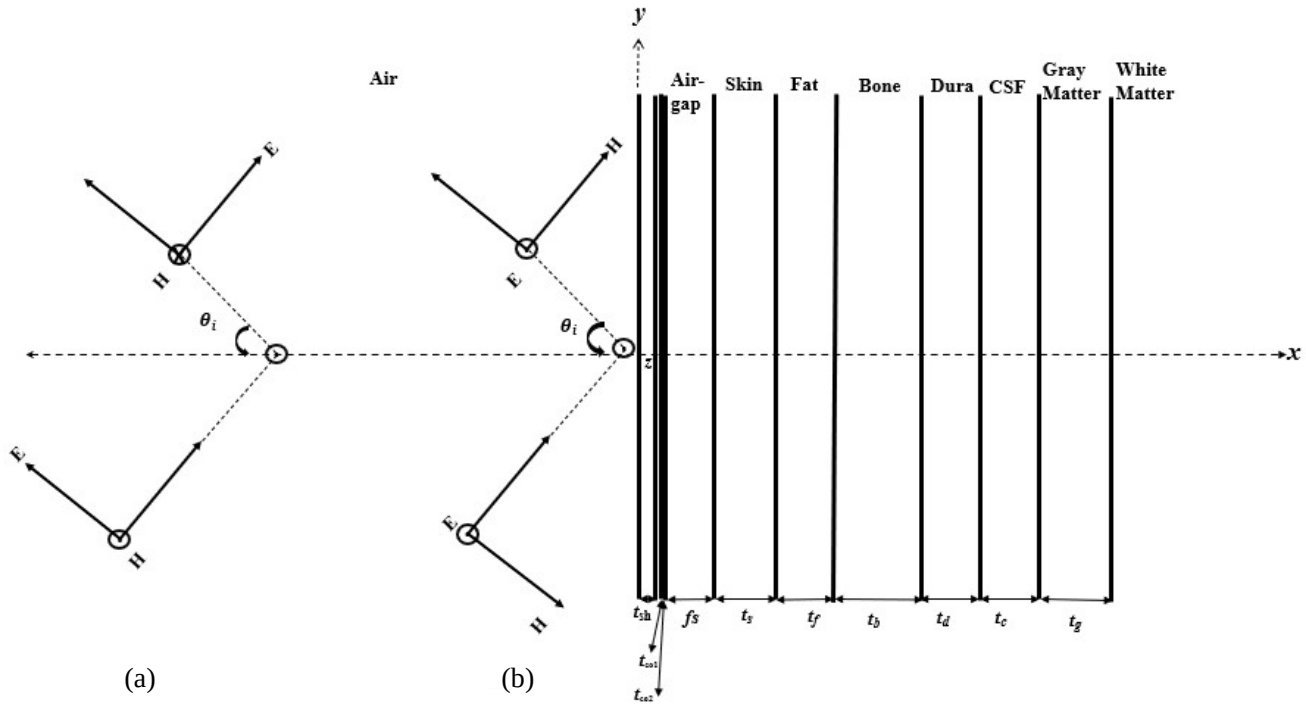

Figure 2. (a) Parallel (TM) Polarization. (b) Perpendicular (TE) Polarization of EM wave incident on air to laminated mesh surface in a planar seven-layered model of adult/child. t_{sh} is PET film thickness and t_{co1}, and t_{co2} are two conductive mesh coatings, seem to be overlapped due to their slight difference in thickness.

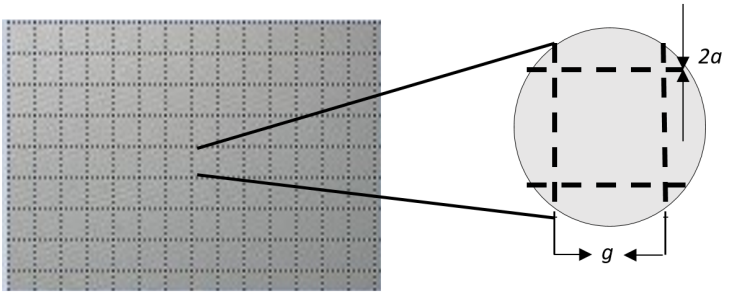

Figure 3. Transparent conductive square mesh coating structure [12].

and an adhesive layer as shown in Fig. 4. The Copper grid and protective Nickel layer are deposited on optical PET film. The transparency of conductive Metal Mesh PET film is tested and achieves more than 80%. The conductive layers possess high flexibility, durability, extremely low resistance, and easy process-ability. The properties of transparent PET film with conductive mesh coatings used in the proposed work are listed in Table 3 [13].

2.4. Head Models with Polarization and Inclusion of Mobile Phone Position

The mobile phone position can be changed from the usual phone holding position according to user (adult/child's) convenience. The two cases of mobile phone holding could be in elevation (vertical) or azimuth (horizontal) direction. There can be two possibilities of shifting the phone in each of the

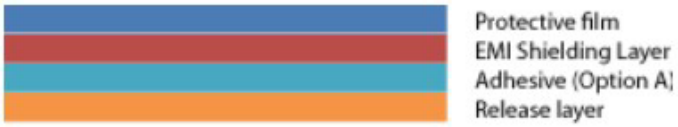

Figure 4. Transparent EMI shielding copper grid PET film [12].

Table 3. Properties of PET film and metal mesh coatings forming a transparent laminated mesh.

Material	Conductivity (S/m)	Thickness	Relative Permittivity	Relative Permeability
PET film	1e-11	100 µm	3.4	1
Cu mesh coating	5.96e7	100 nm	1	1
Ni mesh coating	1.43e7	50 nm	1	100

mentioned mobile phone holding cases. In the elevation direction, the orientation of the mobile phone can be either towards the ear labeled as Position A or away from the ear labeled as Position B. Similarly, in the azimuth direction, the phone positions can be oriented either towards the cheek (Position A) or away from the cheek (Position B). Further understanding of the mobile positions are depicted in Figs. 5, 6, 7 and 8.

Assume that the mobile phone is placed to the right side of the user's head. The head is assumed to be in the first and fourth quadrants of the coordinate plane. Then, the mobile phone is assumed to be situated in the second and third quadrants. Moreover, assuming that the head plane $(x_h y_h)$ is parallel to the coordinate plane (xy) and the user holding the mobile phone plane is $(x_m y_m)$. Supposing that the user shifts the phone position in a tilted $(x_t y_t)$ plane closer to the ear as in Figs. 5 and 6. The mobile is tilted to 15° and 30° elevation direction towards the user's ear (Position A) or away from the ear (Position B), represented with θ_m. In Position A (Position B), if θ_m is measured in clockwise(anti-clockwise) direction with respect to the coordinate y-axis, then the value of elevation angle is negative(positive) θ_m. In Position A (Position B), if θ_m is measured in anti-clockwise(clockwise)

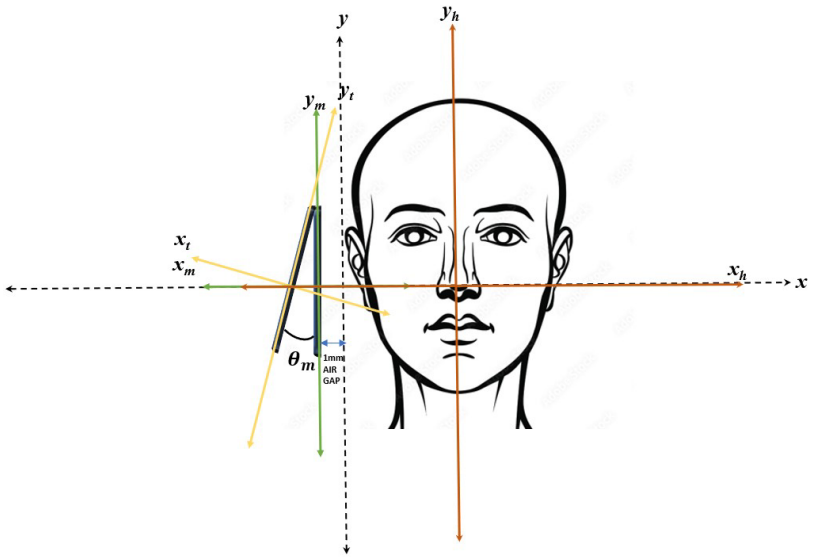

Figure 5. Representation of user (adult/child) holding mobile phone in Position A at 15° and 30° movement towards the ear.

direction with respect to the coordinate y-axis, then the value of elevation angle is positive(negative) θ_m. A differential air gap arises when user tilts the mobile phone. Nevertheless, a 1 mm air gap is considered between the mobile phone plane $(x_m y_m)$ and coordinate plane (xy). In order to maintain the same 1 mm gap even after the shift, the tilted plane $(x_t y_t)$ has to be projected to the usual mobile plane $(x_m y_m)$. Consequently, the impedance of shield and mesh coatings mounted on the handset is modified according to the adjacent impedance component, $\cos\theta_m$.

The mobile is now oriented in the horizontal plane or azimuth direction. In addition to the usual plane of axis, an additional horizontal z-plane comes into the picture. Assuming that the head axis plane $(x_h y_h z_h)$ is coincident with the co-ordinate plane (xyz), shown with dotted lines in Fig. 7 and Fig. 8. Suppose that user holds the mobile phone in the plane $(x_m y_m z_m)$. Let the user shift the mobile phone in the tilted plane $(x_t y_t z_t)$. Now, the phone sweeps an angle ϕ_m in the azimuth direction

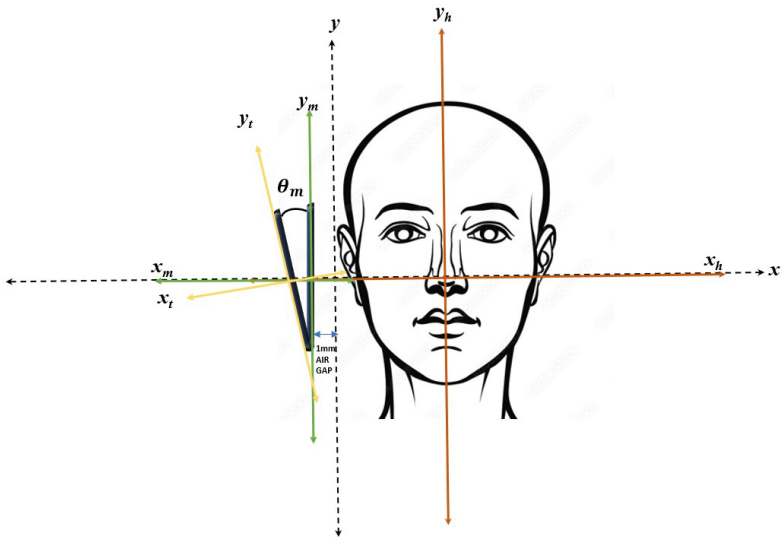

Figure 6. Representation of user(adult/child) holding mobile phone in Position B at 15° and 30° movement away from the ear.

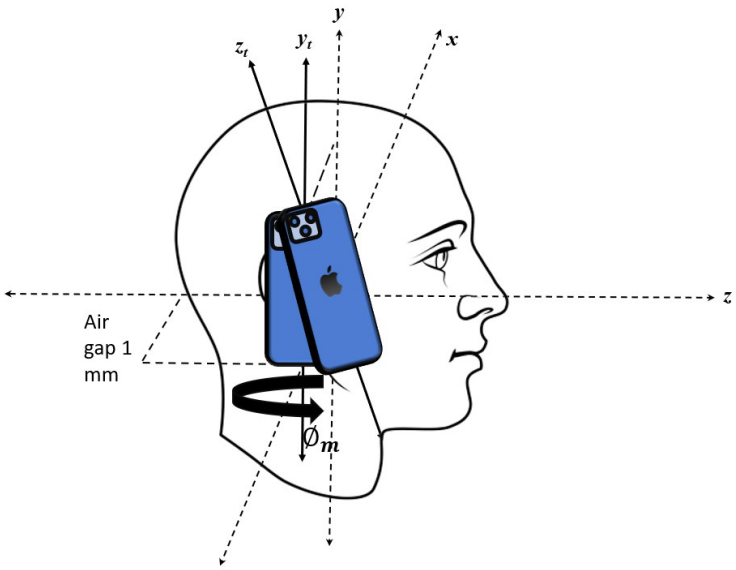

Figure 7. Representation of user (adult/child) holding mobile phone in Position A at 15° and 30° towards the cheek.

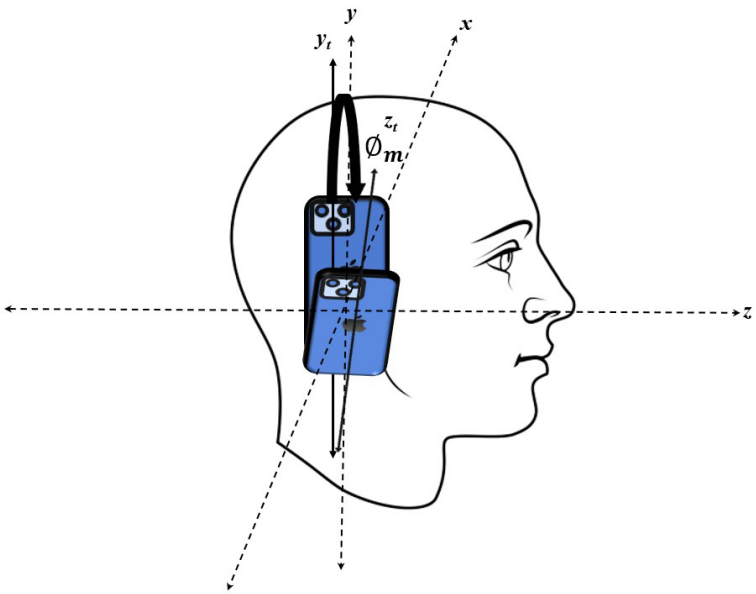

Figure 8. Representation of user (adult/child) holding mobile phone in Position B at 15° and 30° away from the cheek.

for the corresponding θ_m. A 1 mm gap distance is considered between the usual phone holding plane $(x_m y_m z_m)$ and the head. The tilted plane $(x_t y_t z_t)$ in which the mobile phone is now situated, is projected to the usual phone holding plane $(x_m y_m z_m)$ plane such that the impedance of shield and mesh coatings mounted on the mobile handset is changed by the $\cos\phi_m$ factor. Since the adjacent or cos component of the impedance is projected onto the plane in which the mobile phone is situated, no difference in the overall impedance of PET film/TCMCs is observed whether the phone is tilted in elevation/azimuth direction due to the even functionality of cos function. Hence, in any mobile position (Position A or B), only phone tilts are practicable (15° and 30°).

3. MATHEMATICAL FORMULATION OF ESE ALONG WITH OBLIQUE ANGLE OF INCIDENCE AND MOBILE PHONE POSITION INCLUSION

3.1. Impedance of Transparent Conductive Mesh Coatings

The overall impedance of a transparent conductive mesh medium can be categorized in terms of frequency-dependent mesh resistance (R) and reactance (X) in general. Keeping the ratio of mesh period to line width ($\frac{g}{2a}$) in view, the resistance and reactance in (ohms) is derived [14] to be:

$$\begin{aligned} R_{Co} &= \frac{1}{\sigma\delta\left(1-e^{-\frac{t}{\delta}}\right)}\left(\frac{g}{2a}\right) \\ X_{Co} &= \eta_0\left(-\frac{g}{\lambda}\right)\left[\ln\left(\sin\frac{a\pi}{g}\right)\right] \\ Z_{Co} &= \frac{1}{\eta_0}(R_{Co}+iX_{Co}) \end{aligned} \tag{5}$$

where, R_{Co}, X_{Co}, and Z_{Co} are resistance, reactance and total impedance of mesh coating. λ is wavelength of EM wave, δ is the skin depth of continuous conductive mesh coatings (Cu/Ni). t is thickness of mesh.

3.2. Polarized Impedance Equations of PET Film and Transparent Conductive Mesh Coating

The overall complex impedance for both the TCMCs is realized by considering dissimilarities in resistances due to differences in conductivity, skin depth, and thickness of Cu and Ni metal meshes and similarities in reactance due to same mesh parameters. The polarized impedance of shield for insulator [15] and TCMCs are constructed as the following:

$$Z_{sh} = \frac{\left[\sqrt{\frac{\mu_{sh}}{\varepsilon_{sh}}}\right]}{\cos(\theta_{sh})} \tag{6}$$

$$Z_M = \frac{\left[\frac{1}{Z_1}(R_{Co} + iX_{Co})\right]}{\cos(\theta_{Co})} \tag{7}$$

$$Z_1 = \frac{\eta_0}{\cos(\theta_0)} \tag{8}$$

where, Z_{sh} in (6) is TE polarized impedance of PET film as shield. $\cos(\theta_{sh})$ is the angle of refraction of EM wave emerging out of PET film. Z_M in (7) is the TE polarized impedance of Cu and Ni mesh, proportional to R_{Co}, X_{Co}, and $\cos(\theta_{Co})$. Z_1 in (8) is the TE polarized impedance in free space. $\cos\theta_0$ is angle of refraction of EM wave after emerging out of free space medium. The same set of equations is expressed for TM polarized condition, with $Z_1 = \eta_0 \cos\theta_0$ in the numerator. The formulae for angles of refraction, wave numbers, and the dielectric properties of each layered medium are referred from [16].

3.3. Polarized Impedance Equations of PET Film and Transparent Conductive Mesh Coating with Mobile Tilt

When the mobile is shifted to (15° and 30°) tilt position in either elevation or azimuth direction (θ_m or ϕ_m), the impedance of shield and the TCMCs is modified for adjacent component of impedance projection as:

$$Z_{sh} = \frac{\left[\sqrt{\frac{\mu_{sh}}{\varepsilon_{sh}}}\right]\cos(\theta_m)}{\cos(\theta_{sh})} \tag{9}$$

$$Z_M = \frac{\left[\left[\frac{1}{Z_1}(R_{Co} + iX_{Co})\right]\cos(\theta_m)\right]}{\cos(\theta_{Co})} \tag{10}$$

where the polarized impedance of PET film and mesh coatings are now modified along with $\cos(\theta_m)$ in the elevation direction or $\cos(\phi_m)$ in the azimuth direction. The Eqs. (9) and (10) represent the impedance of PET film and TCMC according to phone tilt in TE Polarization. Similarly, equations for the impedance of PET film and TCMCs are written for TM Polarization.

3.4. Formulation of Electromagnetic Shielding Effectiveness and Numerical Assessment of Specific Absorption Rate

The impedance for each layered medium along with impedance of film and mesh Z_{sh} and Z_M are substituted in the reflection coefficients, input impedance, and transmission coefficient of individual seven tissues of HMs and that of shield and TCMCs are derived. The total transmission coefficient T of the radiated EM wave emerging out of transparent PET/Cu/Ni Laminated Mesh and entering the WM tissue taking Figs. 1 and 2 as Reference [17] is:

$$T = p\Big[\left(1 - q_{aSh}e^{-2\gamma_{Sh}t_{sh}}\right)\left(1 - q_{ShC1}e^{-2\gamma_{C1}t_{co1}}\right)\left(1 - q_{C1C2}e^{-2\gamma_{C2}t_{co2}}\right)$$
$$\left(1 - q_{C2a}e^{-2\gamma_{fs}fs}\right)\left(1 - q_{as}e^{-2\gamma_s t_s}\right)\left(1 - q_{sf}e^{-2\gamma_f t_f}\right)$$

$$\left(1-q_{fb}e^{-2\gamma_b t_b}\right)\left(1-q_{bd}e^{-2\gamma_d t_d}\right)\left(1-q_{dc}e^{-2\gamma_c t_c}\right)\left(1-q_{cg}e^{-2\gamma_g t_g}\right)\Bigg]^{-1}$$
$$e^{(-\gamma_{Sh}t_{sh}-\gamma_{C1}t_{co1}-\gamma_{C2}t_{co2}-\gamma_{fs}fs-\gamma_s t_s-\gamma_f t_f-\gamma_b t_b-\gamma_d t_d-\gamma_c t_c-\gamma_g t_g)} \tag{11}$$

where p is the transmission coefficient of wave originating from free-space, transmitting through the intermediate layers and penetrating the WM tissue. q_{aSh}, q_{ShC1}, q_{C1C2}, q_{C2a}, q_{as}, q_{sf}, q_{fb}, q_{bd}, q_{dc}, q_{cg} are reflection coefficients at the interfaces of air-PET film, PET film-Cu coating, Cu coating-Ni coating, Ni coating-air, air-skin, skin-fat, fat-bone, bone-dura, dura-CSF, CSF-gray matter, respectively. γ_{Sh}, γ_{C1}, γ_{C2}, γ_{fs}, γ_s, γ_f, γ_b, γ_d, γ_c, γ_g are propagation constants of wave in each of shield, i.e., PET film, coating 1 and 2, i.e., Cu and Ni layers, free space, skin, fat, bone, dura, CSF, and gray matter, respectively. The thickness of PET film and transparent mesh coatings are represented with t_{sh}, t_{co1}, and t_{co2} as shown in Fig. 2. From T, employing the Transmission Line Method, the ESE in dB is derived for HMs without and with the transparent PET/Cu/Ni LM for the two cases of OAI alone and OAI and mobile position included as:

$$\text{ESE} = -20\log_{10}|T| \tag{12}$$

The ESE in general, applying electric field strength inside the material is:

$$\text{ESE} = 20\log_{10}\left(\frac{E_i}{E_t}\right) \tag{13}$$

The Specific Absorption Rate (SAR) absorbed by the WM tissue of the head is assessed at four fixed Sub-6 GHz 5G frequencies for five oblique angles of incidence (0°, 30°, 45°, 60°, and 89°) in TE and TM Polarization. The assessment is performed without Laminated Mesh, with the LM considering only OAI, with the LM considering both OAI and mobile phone tilts at 15° and 30°. The incident electric field (E_i) is obtained using the power density of the incident EM wave (40 W/m^2) at frequencies above 2 GHz, according to ICNIRP regulations of SAR limiting local exposure applicable to limbs and head [18]. By (13), E_t is calculated for every ESE value obtained at that incident angle at a particular frequency. E_t is the transmitted electric field emitting out of the PET/Cu/Ni laminated mesh and that penetrating WM. The Specific Absorption Rate in (W/kg) is assessed using (14).

$$\text{SAR} = \frac{\sigma_w E_t^2}{\rho_w} \tag{14}$$

Here, σ_w and ρ_w are water-content dependent conductivity (S/m) and tissue mass density of WM, respectively. The value of ρ_w is 1073 kg/m^3 [19, 20].

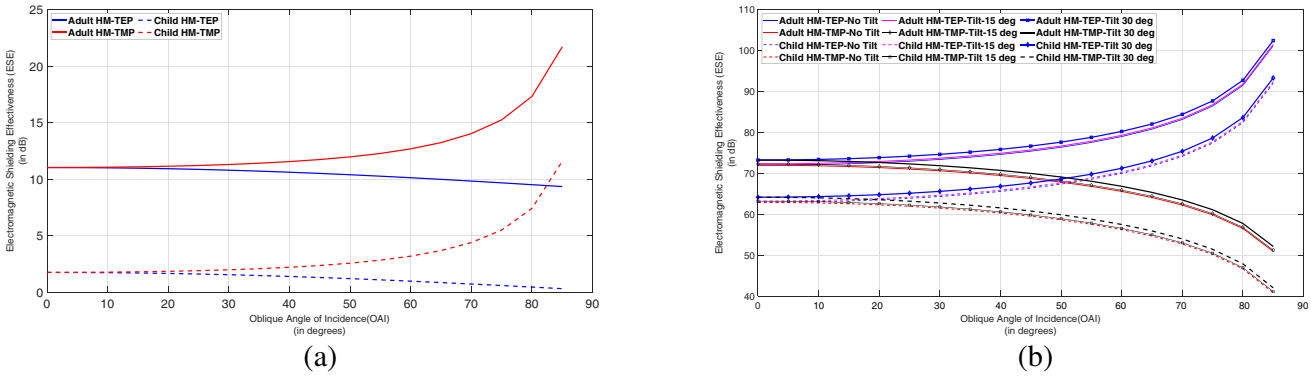

Figure 9. Electromagnetic Shielding Effectiveness (ESE) simulation against Oblique Angle of Incidence (OAI) for TE and TM Polarization (TEP and TMP) in seven-layered adult and child head models (HMs). (a) Without transparent PET/Cu/Ni Laminated Mesh (LM), and without mobile phone tilt at 2.3 GHz. (b) With transparent PET/Cu/Ni Laminated Mesh (LM) before and after mobile phone 15° and 30° tilt at 2.3 GHz.

4. RESULTS AND DISCUSSION

4.1. Electromagnetic Shielding Effectiveness Simulation of Adult and Child Head Models without Transparent PET/Cu/Ni Laminated Mesh

Since the shield (PET film) and coating impedance (Cu and Ni) are projected parallel to the head axis, without any shield placement, there is no change in ESE, which means that the ESE before and after the mobile phone tilt remained the same. The simulations of ESE at four 5G frequencies, 2.3 GHz, 3.6 GHz, 4.5 GHz, and 5.47 GHz, are performed for adult and child HMs for variation with OAI from 0° to 90° in TE and TM Polarization. The ESE simulation of HMs when LM is not used as an external shield is shown in Figs. 9(a), 10(a), 11(a), and 12(a) for TE and TM Polarization of EM radiated wave. The ESE is more in TM Polarization direction than TE Polarization when the transparent PET/Cu/Ni LM is not used. The variation in shielding effectiveness with each incident angle is minimal in TE compared to TM Polarization, because symmetry is not observed in TE Polarization. Also, the gap between the TE and TM Polarization curves keeps decreasing as 5.47 GHz is approached.

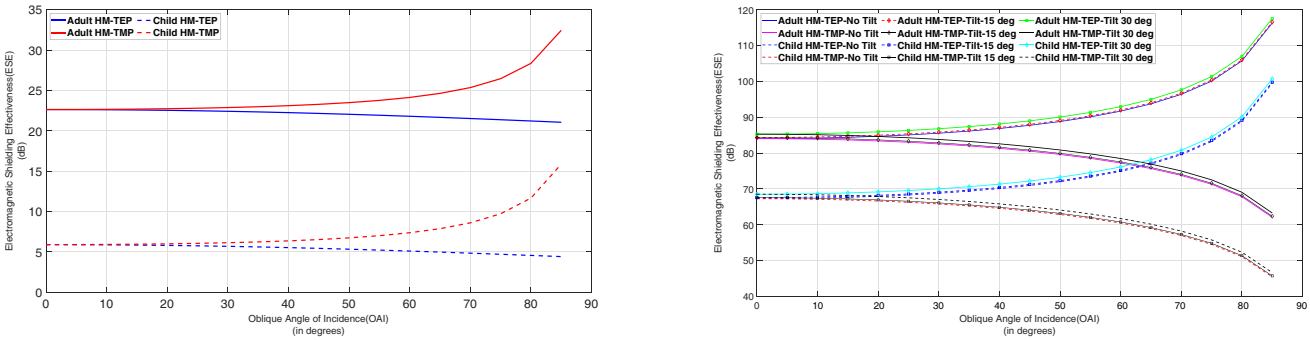

(a) (b)

Figure 10. Electromagnetic Shielding Effectiveness (ESE) simulation against Oblique Angle of Incidence (OAI) for TE and TM Polarization (TEP and TMP) in seven-layered adult and child head models (HMs). (a) Without transparent PET/Cu/Ni Laminated Mesh (LM), and without mobile phone tilt at 3.6 GHz. (b) With transparent PET/Cu/Ni Laminated Mesh (LM) before and after mobile phone 15° and 30° tilt at 3.6 GHz.

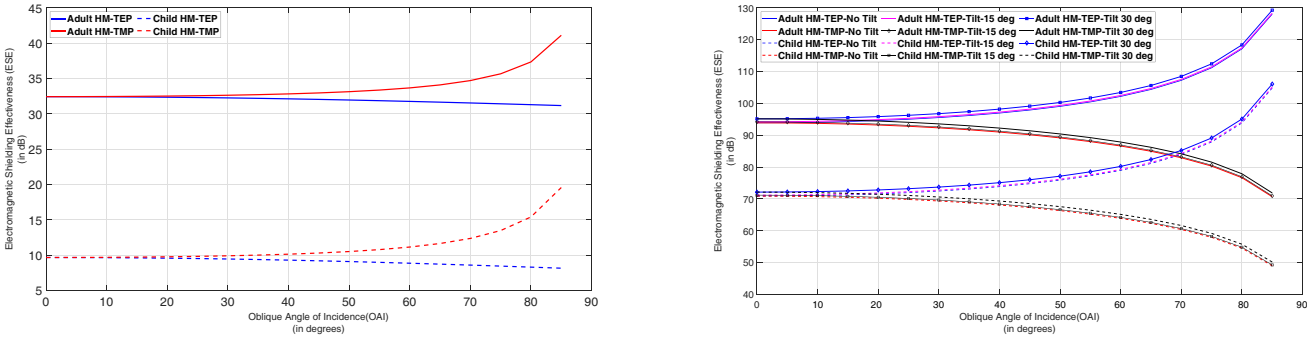

(a) (b)

Figure 11. Electromagnetic Shielding Effectiveness (ESE) simulation against Oblique Angle of Incidence (OAI) for TE and TM Polarization (TEP and TMP) in seven-layered adult and child head models (HMs). (a) Without transparent PET/Cu/Ni Laminated Mesh (LM), and without mobile phone tilt at 4.5 GHz. (b) With transparent PET/Cu/Ni Laminated Mesh (LM) before and after mobile phone 15° and 30° tilt at 4.5 GHz.

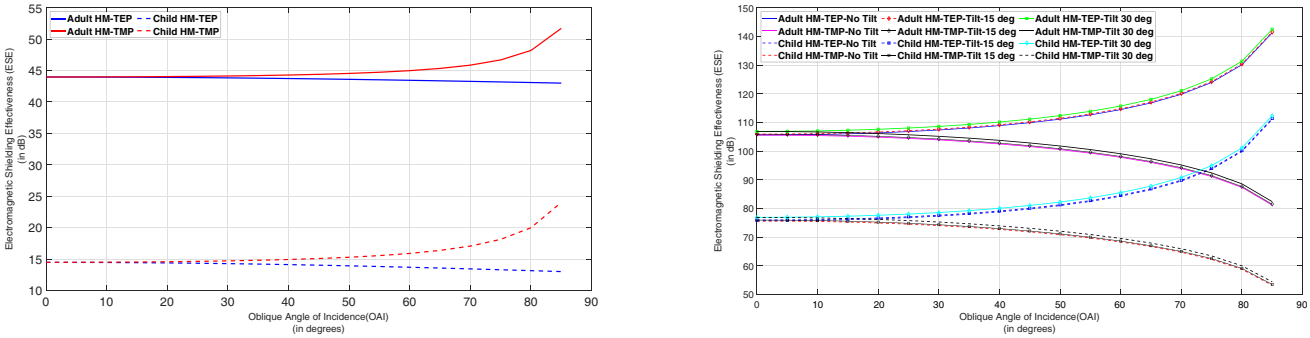

Figure 12. Electromagnetic Shielding Effectiveness (ESE) simulation against Oblique Angle of Incidence (OAI) for TE and TM Polarization (TEP and TMP) in seven-layered adult and child head models (HMs). (a) Without transparent PET/Cu/Ni Laminated Mesh (LM), and without mobile phone tilt at 5.47 GHz. (b) With transparent PET/Cu/Ni Laminated Mesh (LM) before and after mobile phone 15° and 30° tilt at 5.47 GHz.

4.2. Electromagnetic Shielding Effectiveness Simulation of Adult and Child Head Models with Transparent PET/Cu/Ni Laminated Mesh, without and with Mobile Phone Tilt

With transparent PET/Cu/Ni laminated mesh, the ESE deviation with the incident angles (0° to 90°) is observed in adult and child HMs for two cases. The first case is when the mobile phone tilt is not considered. In the second case, when mobile phone tilt of 15 and 30° is considered. From the simulation graphs in Figs. 9(b), 10(b), 11(b), and 12(b), one common study that can be made is the ESE of adult HM with the LM is more than the child HM. ESE in TE and TM Polarization in adult HM is more than ESE in child HM. Furthermore, a mobile phone tilt of 30° in adult/child HM achieved higher ESE than the mobile phone tilt of 15° and no tilt condition in perpendicular/parallel polarization. At an incident angle of 85° from the plot, the ESE in perpendicular and parallel polarization in adult HM achieved is 102 dB and 51 dB at 2.3 GHz, respectively. By child HM, the ESE obtained is 93 dB(41 dB) in TE(TM) Polarization. Similarly, at 5.47 GHz and 85° angle of incidence, the adult HM achieved 142 dB(82 dB) in TE(TM) Polarization. The child HM achieved shielding effectiveness of 112 dB(53.49 dB) in TE(TM) Polarization.

4.3. Specific Absorption Rate Assessment using Electromagnetic Shielding Effectiveness Simulations Numerically

A numerical assessment of the Specific Absorption Rate absorbed by White Matter (WM) is performed based on the ESE divergence with the angle of incidence and mobile position in adult and child human HMs at 5G frequencies. The assessment is performed in TE and TM Polarization with transparent PET/Cu and Ni laminated mesh. The tissue absorption of SAR in both the HMs is represented and compared.

The comparisons from Tables 4 and 5 states that in the usual mobile position at 2.3 GHz for adult HM, in TE and TM Polarization, tissue WM absorbed a SAR as high as 5.124 W/kg for 0° OAI with no transparent PET/Cu/Ni LM. The SAR increased to 7.7 W/kg at 89° in TE Polarization and decreased to 0.0243 W/kg in TM Polarization. The child HM absorbed an EM energy without the shield as high as 42 W/kg, which is increased to 60.2 W/kg and decreased to 0.25 W/kg in TE and TM Polarization, respectively. The adult's WM in TE and TM Polarization using PET/Cu/Ni LM absorbed a SAR of 0.0000041 W/kg at normal incidence, decreased to 1.28e-11 W/kg at 89° in TEP; and increased to 0.00548 W/kg in TMP. The child's WM in TE and TM Polarization using PET/Cu/Ni LM absorbed a SAR of 0.000032 W/kg at normal incidence, decreased to 1e-10 W/kg at 89° in TEP; and increased to 0.0575 W/kg in TMP.

Using the laminated mesh, with a 15° (in either elevation/azimuth direction) mobile phone tilt, the same WM of adult absorbed a SAR of 0.00000383 W/kg at 0° angle of incidence in TEP and decreased

Table 4. Comparison of SAR (W/kg) by the White Matter (WM) tissue in Adult HM without and with transparent PET/Cu/Ni Laminated Mesh (LM). The incident angles are considered for TE and TM Polarization (TEP and TMP) with and without mobile phone tilt (elevation/azimuth) at 2.3 GHz.

Angle of Incidence (Deg)	SAR before Mobile Phone tilt (W/kg)				SAR after 15° Mobile Phone tilt (W/kg)		SAR after 30° Mobile Phone tilt (W/kg)	
	No Shield in TEP	No Shield in TMP	PET /Cu /Ni LM in TEP	PET /Cu /Ni LM in TMP	PET /Cu /Ni LM in TEP	PET /Cu /Ni LM in TMP	PET /Cu /Ni LM in TEP	PET /Cu /Ni LM in TMP
0	5.124	5.124	4.10E-06	4.10E-06	3.83E-06	3.83E-06	3.08E-06	3.08E-06
30	5.41	4.819	2.97E-06	5.63E-06	2.78E-06	5.25E-06	2.23E-0	4.22E-06
45	5.779	4.354	1.87E-06	8.70E-06	1.75E-06	8.12E-06	1.41E-06	6.53E-06
60	6.307	3.506	8.22E-07	1.79E-05	7.67E-07	1.67E-05	6.17E-07	1.34E-05
89	7.786	0.0243	1.28E-11	0.00548	1.19E-11	0.00519	9.60E-12	0.00439

Table 5. Comparison of SAR (W/kg) by the White Matter (WM) tissue in Child HM without and with transparent PET/Cu/Ni Laminated Mesh (LM). The incident angles are considered for TE and TM Polarization (TEP and TMP) with and without mobile phone tilt (elevation/azimuth) at 2.3 GHz.

Angle of Incidence (Deg)	SAR before Mobile Phone tilt (W/kg)				SAR after 15° Mobile Phone tilt (W/kg)		SAR after 30° Mobile Phone tilt (W/kg)	
	No Shield in TEP	No Shield in TMP	PET /Cu /Ni LM in TEP	PET /Cu /Ni LM in TMP	PET /Cu /Ni LM in TEP	PET /Cu /Ni LM in TMP	PET /Cu /Ni LM in TEP	PET /Cu /Ni LM in TMP
0	42.136	42.136	3.22E-05	3.22E-05	3.00E-05	3.00E-05	2.41E-05	2.41E-05
30	44.152	39.944	2.32E-05	4.45E-05	2.16E-05	4.16E-05	1.74E-05	3.34E-05
45	46.715	36.589	1.45E-05	6.99E-05	1.35E-05	6.52E-05	1.09E-05	5.25E-05
60	50.356	30.252	6.34E-06	1.49E-04	5.91E-06	1.39E-04	4.75E-06	1.12E-04
89	60.208	0.256	1.00E-10	0.0575	9.34E-11	0.0545	7.51E-11	0.0461

at 89° to 1.19e-11 W/kg; it is increased to 0.00519 W/kg at the same incident angle in TMP. With the same 15° tilt, the HM of a child imbibed a SAR of 0.00003 W/kg at normal incidence in TE Polarization. However, the energy absorbed decreased to a minimum value of 9.34e-11 W/kg. The absorption rate is raised to 0.05 W/kg at 89° TM Polarization, using the PET/Cu and Ni LM. With a 30° mobile phone tilt, the HMs absorbed a slightly lower SAR of 0.00000306 W/kg and 0.000024 W/kg at 0° in TEP in adult and child's WM, respectively, than with the 15° tilt at normal incidence. The SAR absorption by WM tissue is reduced to a negligible value of 9.6e-12 W/kg and 7.5e-11 W/kg in 89° TEP in adult and child HMs, respectively. In contrast to TE Polarization, the same HM in the adult and child absorbed

a much higher 0.00439 W/kg and 0.0461 W/kg radiation from the mobile phone at the same incident angle TMP, respectively, with the laminated mesh.

Comparisons from tables show that the ESE of human adult and child HMs at 3.6 GHz, 4.5 GHz, and 5.47 GHz has absorbed much lower radiation in TEP than at 2.3 GHz when the transparent laminated mesh is considered. The reduction in SAR is more at 3.6 GHz by the adult's white matter, which is 0.6(0.9) W/kg at 0°(89°) TEP because of inverse logarithmic proportionality of ESE with SAR. The ESE achieved is as high as around 115 dB by adult HM at 0° TEP. A similar comparison chart can be drawn between the Tables 6, 7, and 8, 9.

Table 6. Comparison of SAR (W/kg) by the White Matter (WM) tissue in Adult HM without and with transparent PET/Cu/Ni Laminated Mesh (LM). The incident angles are considered for TE and TM Polarization (TEP and TMP) with and without mobile phone tilt (elevation/azimuth) at 3.6 GHz.

Angle of Incidence (Deg)	**SAR before Mobile Phone tilt (W/kg)**				**SAR after 15° Mobile Phone tilt (W/kg)**		**SAR after 30° Mobile Phone tilt (W/kg)**	
	No Shield in TEP	**No Shield in TMP**	**PET /Cu /Ni LM in TEP**	**PET /Cu /Ni LM in TMP**	**PET /Cu /Ni LM in TEP**	**PET /Cu /Ni LM in TMP**	**PET /Cu /Ni LM in TEP**	**PET /Cu /Ni LM in TMP**
0	0.607	0.607	4.41E-07	4.41E-07	4.12E-07	4.12E-07	3.31E-07	3.31E-07
30	0.638	0.573	3.12E-07	6.20E-07	2.91E-07	5.78E-07	2.34E-07	4.65E-07
45	0.677	0.523	1.88E-07	9.85E-07	1.76E-07	9.19E-07	1.41E-07	7.39E-07
60	0.735	0.429	7.56E-08	2.11E-06	7.05E-08	1.97E-06	5.67E-08	1.58E-06
89	0.898	0.0038	5.56E-13	0.00074	5.19E-13	0.0007	4.17E-13	0.0006

Table 7. Comparison of SAR (W/kg) by the White Matter (WM) tissue in child HM without and with transparent PET/Cu/Ni Laminated Mesh (LM). The incident angles are considered for TE and TM Polarization (TEP and TMP) with and without mobile phone tilt (elevation/azimuth) at 3.6 GHz.

Angle of Incidence (Deg)	**SAR before Mobile Phone tilt (W/kg)**				**SAR after 15° Mobile Phone tilt (W/kg)**		**SAR after 30° Mobile Phone tilt (W/kg)**	
	No Shield in TEP	**No Shield in TMP**	**PET /Cu /Ni LM in TEP**	**PET /Cu /Ni LM in TMP**	**PET /Cu /Ni LM in TEP**	**PET /Cu /Ni LM in TMP**	**PET /Cu /Ni LM in TEP**	**PET /Cu /Ni LM in TMP**
0	27.574	27.574	2.02E-05	2.02E-05	1.89E-05	1.89E-05	1.52E-05	1.52E-05
30	28.933	26.105	1.43E-05	2.83E-05	1.33E-05	2.64E-05	1.07E-05	2.13E-05
45	30.662	23.862	8.66E-06	4.50E-05	8.08E-06	4.20E-05	6.49E-06	3.38E-05
60	33.121	19.643	3.51E-06	9.65E-05	3.27E-06	9.01E-05	2.63E-06	7.25E-05
89	39.829	0.161	2.49E-11	0.031	2.33E-11	0.0295	1.87E-11	0.0251

Table 8. Comparison of SAR (W/kg) by the White Matter (WM) tissue in adult HM without and with transparent PET/Cu/Ni Laminated Mesh (LM). The incident angles are considered for TE and TM Polarization(TEP and TMP) with and without mobile phone tilt (elevation/azimuth) at 4.5 GHz.

Angle of Incidence (Deg)	SAR before Mobile Phone tilt (W/kg)				SAR after 15° Mobile Phone tilt (W/kg)		SAR after 30° Mobile Phone tilt (W/kg)	
	No Shield in TEP	No Shield in TMP	PET /Cu /Ni LM in TEP	PET /Cu /Ni LM in TMP	PET /Cu /Ni LM in TEP	PET /Cu /Ni LM in TMP	PET /Cu /Ni LM in TEP	PET /Cu /Ni LM in TMP
0	0.087	0.0874	6.24E-08	6.24E-08	5.82E-08	5.82E-08	4.68E-08	4.68E-08
30	0.091	0.0834	4.29E-08	8.98E-08	4.00E-08	8.38E-08	3.22E-08	6.74E-08
45	0.0955	0.0774	2.49E-08	1.48E-07	2.32E-08	1.38E-07	1.86E-08	1.11E-07
60	0.102	0.0657	9.28E-09	3.33E-07	8.66E-09	3.11E-07	6.96E-09	2.50E-07
89	0.119	0.000787	4.76E-14	0.000143	4.44E-14	0.000136	3.57E-14	0.000117

Table 9. Comparison of SAR (W/kg) by the White Matter (WM) tissue in child HM without and with transparent PET/Cu/Ni Laminated Mesh (LM). The incident angles are considered for TE and TM Polarization (TEP and TMP) with and without mobile phone tilt (elevation/azimuth) at 4.5 GHz.

Angle of Incidence (Deg)	SAR before Mobile Phone tilt (W/kg)				SAR after 15° Mobile Phone tilt (W/kg)		SAR after 30° Mobile Phone tilt (W/kg)	
	No Shield in TEP	No Shield in TMP	PET /Cu /Ni LM in TEP	PET /Cu /Ni LM in TMP	PET /Cu /Ni LM in TEP	PET /Cu /Ni LM in TMP	PET /Cu /Ni LM in TEP	PET /Cu /Ni LM in TMP
0	15.827	15.827	1.19E-05	1.19E-05	1.11E-05	1.11E-05	8.96E-06	8.96E-06
30	16.425	14.976	8.31E-06	1.70E-05	7.75E-06	1.59E-05	6.23E-06	1.27E-05
45	17.624	13.681	4.89E-06	2.74E-05	4.56E-06	2.56E-05	3.67E-06	2.06E-05
60	19.068	11.257	1.86E-06	5.96E-05	1.74E-06	5.56E-05	1.40E-06	4.48E-05
89	23.052	0.0957	9.27E-12	0.0175	8.65e-12	0.0165	6.96E-12	0.013

From Tables 10 and 11, at the mobile 5.47 GHz frequency in the adult head, the SAR absorbed by brain WM has reduced excessively from 4.22e-09 W/kg at normal incidence to 2.17e-15 W/kg at 89° in TE Polarization with 30° mobile phone tilt in elevation or azimuth direction using transparent PET/Cu/Ni laminated mesh. The child head's WM has imbibed in a much higher SAR of 0.000004 W/kg at 0° in TEP compared to the adult head's WM. At 89°, the radiation absorption reduction is as lower than 2.1e-12 W/kg at 30° tilt. In TMP, with the same laminated mesh, the SAR absorbed by the adult WM has enlarged to 0.0000139 W/kg at 89°. It is increased to 0.00692 W/kg at 89° in child HM. Tilting the adult's mobile position to 15° with the LM has reduced the absorption

Table 10. Comparison of SAR (W/kg) by the White Matter (WM) tissue in adult HM without and with transparent PET/Cu/Ni Laminated Mesh (LM). The incident angles are considered for TE and TM Polarization (TEP and TMP) with and without mobile phone tilt (elevation/azimuth) at 5.47 GHz.

Angle of Incidence (Deg)	SAR before Mobile Phone tilt (W/kg)				SAR after 15° Mobile Phone tilt (W/kg)		SAR after 30° Mobile Phone tilt (W/kg)	
	No Shield in TEP	No Shield in TMP	PET /Cu /Ni LM in TEP	PET /Cu /Ni LM in TMP	PET /Cu /Ni LM in TEP	PET /Cu /Ni LM in TMP	PET /Cu /Ni LM in TEP	PET /Cu /Ni LM in TMP
0	0.0082	0.00821	5.63E-09	5.63E-09	5.25E-09	5.25E-09	4.22E-09	4.22E-09
30	0.0085	0.00792	3.77E-09	8.32E-09	3.51E-09	7.77E-09	2.83E-09	6.24E-09
45	0.0088	0.00744	2.10E-09	1.42E-08	1.96E-09	1.32E-08	1.57E-09	1.06E-08
60	0.00927	0.00651	7.33E-10	3.38E-08	6.84E-10	3.15E-08	5.50E-10	2.54E-08
89	0.0104	9.72E-05	2.89E-15	1.69E-05	2.69E-15	1.61E-05	2.17E-15	1.39E-05

Table 11. Comparison of SAR (W/kg) by the White Matter (WM) tissue in child HM without and with transparent PET/Cu/Ni Laminated Mesh (LM). The incident angles are considered for TE and TM Polarization (TEP and TMP) with and without mobile phone tilt (elevation/azimuth) at 5.47 GHz.

Angle of Incidence (Deg)	SAR before Mobile Phone tilt (W/kg)				SAR after 15° Mobile Phone tilt (W/kg)		SAR after 30° Mobile Phone tilt (W/kg)	
	No Shield in TEP	No Shield in TMP	PET /Cu /Ni LM in TEP	PET /Cu /Ni LM in TMP	PET /Cu /Ni LM in TEP	PET /Cu /Ni LM in TMP	PET /Cu /Ni LM in TEP	PET /Cu /Ni LM in TMP
0	6.975	6.975	5.32E-06	5.32E-06	4.96E-06	4.96E-06	3.99E-06	3.99E-06
30	7.31	6.614	3.62E-06	7.72E-06	3.37E-06	7.20E-06	5.81E-06	5.79E-06
45	7.738	6.061	2.05E-06	1.28E-05	1.92E-06	1.19E-05	9.62E-06	9.58E-06
60	8.351	5.027	7.33E-07	2.87E-05	6.84E-07	2.68E-05	5.50E-07	2.16E-05
89	10.059	0.048	2.80E-12	0.0084	2.62E-12	8.01E-03	2.10E-12	0.0069

from 5.2e-9 W/kg to a negligible amount of 2.7e-15 W/kg in TEP. The WM's absorption has escalated to 0.000016 W/kg in TMP. Tilting the child's phone position to 15° in either elevation or azimuth direction, the reduction in SAR is seen from 0.000005 W/kg to 2.62e-12 W/kg in TEP. The SAR is comparatively more in TM Polarization from 0.000005 W/kg to 0.008 W/kg. In no tilt condition, using the same laminated LM, the TEP has decreased the SAR absorption by adult WM tissue from 5.63e-9 W/kg to 2.89e-15 W/kg, whereas in TM Polarization, the SAR absorption has raised to 0.000017 W/kg. The child HM, on the other hand, has absorbed the level of radiation from 0.0000053 W/kg at 0° incident angle to 2.8e-12 W/kg at 89° OAI in TEP and surged to 0.0083 W/kg in TMP at 89°. With 15° and

30° tilt, respectively, using the same transparent LM, the SAR absorption is reduced to 4.96e-6 W/kg at normal incidence, whereas the SAR is decreased significantly to 2.62e-12 W/kg and 2.1e-12 W/kg at 89°. In TMP, the child's WM tissue absorbed a relatively higher radiation level of 0.0084 W/kg and 0.007 W/kg for 15° and 30° tilt, respectively, at 89° OAI.

Therefore, from common observation, as frequency is progressed from 2.3 to 5.47 GHz, the specific absorption rate emitted from the mobile phone diminished for no shield condition since the shielding effectiveness of the human head is computed for the mobile phone without a shield as well. The direct proportionality between ESE and frequency variables indirectly affects SAR reduction as the frequency progresses to 5.47 GHz. From the available literature, any child HM absorbed more SAR than any adult HM with varying tissue properties. The same is obtained from the results of the numerical SAR assessment. At maximum incident angle 89° at 5.47 GHz, the SAR absorbed in TE Polarization condition with no shield in a child's white matter layer is around 10 W/kg. The transparent laminated mesh made of optical PET film, Cu, and Ni conductive mesh coating layers minimizes the the absorption amount of mobile radiation to a negligible value of 2.8e-12 W/kg. It is comparatively lesser when the mobile phone is tilted to 15°, which is 2.62e-12 W/kg. Moreover, more comparatively, with a mobile tilt of 30°, the absorption rate is diminished to 2.1e-12 W/kg. The maximum SAR absorption is apparent at normal incidence in TE Polarization and 89° in TM Polarization in both the HMs.

5. CONCLUSION

A detailed theoretical and mathematical investigation is performed on the effect of mobile user position in either elevation or azimuth directions to notice the SAR absorption and to mitigate it by utilizing optically transparent PET film as shield and transparent conductive metal mesh coatings with minimal thickness. Transmission Line Method is used in the proposed work to evaluate the material property of Electromagnetic Shielding Effectiveness for two age-dependent head models in the presence of the user's mobile tilt positions and under the consideration of the oblique angle of incidence of RF EM wave. The mathematical formulation to evaluate the shielding effectiveness with the mobile position consideration and oblique angle of incidence of a plane wave; is performed to estimate the amount of RF radiation penetrating the white matter of the adult/child's head. The results show that the RF radiation emitted from the mobile phone or the SAR penetrated the child's White Matter tissue more. Nevertheless, with the aid of transparent conductive Metal Mesh PET film (transparent PET/Cu/Ni laminated mesh), at a mobile tilt of 30° and 89° TE Polarization, the SAR absorbed by the child's head is the least, which is 2e-12 W/kg when compared with SAR absorbed by child HM with no shield considered which is 10.05 W/kg at 5.47 Sub-6 GHz frequency. Furthermore, the adult model absorbed a least negligible SAR of 2.17e-15 at the same incident angle in TE Polarization when the adult's mobile phone tilt is observed at 30°.

REFERENCES

1. Gultekin, D. H. and P. H. Siegel, "Absorption of 5G radiation in brain tissue as a function of frequency, power and time," *IEEE Access*, Vol. 8, 115593–115612, 2020.
2. Ramachandran, T., M. R. I. Faruque, and M. T. Islam, "Specific absorption rate reduction for sub-6 frequency range using polarization dependent metamaterial with high effective medium ratio," *Scientific Reports*, Vol. 12, No. 1, 1–182, 2022.
3. Sacco, G., S. Pisa, and Z. Maxim, "Age-dependence of electromagnetic power and heat deposition in near-surface tissues in emerging 5G bands," *Scientific Reports*, Vol. 11, No. 1, 1–11, 2021.
4. Lwin, Z. M. and M. Yokota, "Numerical analysis of SAR and temperature distribution in two dimensional human head model based on FDTD parameters and the polarization of electromagnetic wave," *AEU-International Journal of Electronics and Communications*, Vol. 104, 91–98, 2019.
5. Bhargava, D., N. Leeprechanon, et al., "Specific absorption rate and temperature elevation in the human head due to overexposure to mobile phone radiation with different usage patterns," *International Journal of Heat and Mass Transfer*, Vol. 130, 1178–1188, 2019.

6. Iqbal-Faruque, M. R., et al., "Effects of mobile phone radiation onto human head with variation of holding cheek and tilt positions," *Journal of Applied Research and Technology*, Vol. 12, No. 5, 871–876, 2014.
7. Drossos, A., V. Santomaa, and N. Kuster, "The dependence of electromagnetic energy absorption upon human head tissue composition in the frequency range of 300–3000 MHz," *IEEE Transactions on Microwave Theory and Techniques*, Vol. 48, No. 11, 1988–1995, 2000.
8. Rajagopal, B. and L. Rajasekaran, "SAR assessment on three layered spherical human head model irradiated by mobile phone antenna," *Human-centric Computing and Information Sciences*, Vol. 4, No. 1, 1–11, 2014.
9. Hout, S. and J. Y. Chung, "Design and characterization of a miniaturized implantable antenna in a seven-layer brain phantom," *IEEE Access*, Vol. 7, 162062–162069, 2019.
10. Wang, J., O. Fujiwara, and S. Watanabe, "Approximation of aging effect on dielectric tissue properties for SAR assessment of mobile telephones," *IEEE Transactions on Electromagnetic Compatibility*, Vol. 48, No. 2, 408–413, 2006.
11. http://niremf.ifac.cnr.it/docs/DIELECTRIC/AppendixC.html.
12. https://hollandshielding.com/Transparent-EMI-shielding-copper-grid-PET-film.
13. https://www.thoughtco.com/table-of-electrical-resistivity-conductivity-608499.
14. Liu, Y. and J. Tan, "Frequency dependent model of sheet resistance and effect analysis on shielding effectiveness of transparent conductive mesh coatings," *Progress In Electromagnetics Research*, Vol. 140, 353–368, 2013.
15. Ott, H. W., *Electromagnetic Compatibility Engineering*, John Wiley & Sons, 2011.
16. Jayasree, P. V. Y., V. S. S. Baba, B. P. Rao, and P. Lakshman, "Analysis of shielding effectiveness of single, double and laminated shields for oblique incidence of EM waves," *Progress In Electromagnetics Research B*, Vol. 22, 187–202, 2010.
17. Spandana, P. S. and P. V. Y. Jayasree, "Numerical computation of SAR in human head with transparent shields using transmission line method," *Progress In Electromagnetics Research M*, Vol. 105, 31–44, 2021.
18. International Commission on Non-Ionizing Radiation Protection and others, "Guidelines for limiting exposure to electromagnetic fields (100 kHz to 300 GHz)," *Health Physics*, Vol. 118, No. 5, 483–524, 2020.
19. Mohammed, B., K. Bialkowski, A. Abbosh, P. C. Mills, and A. P. Bradley, "Closed-form equation to estimate the dielectric properties of biological tissues as a function of age," *Bioelectromagnetics*, Vol. 38, No. 6, 474–481, 2017.
20. Dutta, P. K., P. V. Y. Jayasree, and V. S. S. N. S. Baba, "SAR reduction in the modelled human head for the mobile phone using different material shields," *Human-centric Computing and Information Sciences*, Vol. 6, No. 1, 1–22, 2016.